

# Topological Quantum Computing

Fabian Hassler

Institute for Quantum Information  
RWTH Aachen University  
Germany

October 2024

## Contents

<b>1</b>	<b>Introduction</b>	<b>2</b>
<b>2</b>	<b>Topological superconductors</b>	<b>3</b>
2.1	Topological quantum number	3
2.2	Kitaev model	5
2.3	Majorana zero modes	6
<b>3</b>	<b>Majorana qubits</b>	<b>7</b>
3.1	Fermionic quantum computation	8
3.2	Encoding of a qubit	9
3.3	Fusion and splitting	10
<b>4</b>	<b>Braiding</b>	<b>11</b>
4.1	Abelian anyons	13
4.2	Ising anyons	13
4.3	Fibonacci anyons	15
<b>5</b>	<b>Conclusion</b>	<b>19</b>
<b>A</b>	<b>Braiding of Majorana zero modes</b>	<b>21</b>
A.1	Non-Abelian Berry phase	22
A.2	Calculation	22
	<b>References</b>	<b>25</b>

# 1 Introduction

The concept of *identical particles* is one of the most counterintuitive features of many-body quantum mechanics, maybe second only to the concept of entanglement. In fact, even the bosonic exchange statistics, which is the closest to our classical world, has puzzled researchers time and time again. The hallmark experiment by Hanbury Brown and Twiss [1], showing two-photon interference, was initially facing strong criticism: Brannen and Ferguson, for example, stated that “it would appear to the authors [...] that if such a correlation did exist, it would call for a major revision of some fundamental concepts in quantum mechanics” [2]. As a reply, Purcell did point out that “the electromagnetic field is a classical field after all, which is why the Brown-Twiss effect only appears odd if one looks at it from a particle point of view; its oddness being simply the *peculiarity of bosons*” [3]. Going over to fermions, we do not even have a classical analog. The basic principle of fermions is that they are described by anticommuting numbers. However, all observables, being part of our everyday classical world, are bosonic. The consistency with quantum mechanics then demands ‘*superselection*’, which means that all observables have to be formed by an even number of fermionic operators.

The idea of using identical particles and their exchange statistics as a resource for quantum computation is only a couple of decades old [4, 5]. The reason is that ‘simple’ fermions and bosons, which we are familiar with from the basic physics courses, are not useful for this task. Researchers have been looking at extensions of the concept of exchange statistics of identical particles beyond the notion of fermions and bosons. However, in three dimensions nothing interesting arises as all possible parastatistics can be reduced to bosons and fermions.<sup>1</sup>

In two dimensions, we know that charged particles (with charge  $q$ ) pick up the Aharonov-Bohm phase  $q\Phi/\hbar$  when encircling a magnetic flux  $\Phi$ . The Aharonov-Bohm phase is *topological* in the sense that it does not depend on the concrete trajectory taken by the particles but only on the winding of the particle around the flux. Composite (bosonic) particles consisting of an electric charge  $q$  and a magnetic flux  $\Phi$  acquire a phase  $\theta = q\Phi/2\hbar$  when exchanged.<sup>2</sup> The value  $\theta = 0$  ( $\theta = \pi$ ) corresponds to a composite boson (fermion). However, also other values are allowed which correspond to Abelian anyons. In three dimensions, the construction does not work. In fact, it is a theorem by Dirac [6] that a consistent theory only allows for pointlike magnetic charges (called magnetic monopoles) that produce a flux of size  $\Phi_0 = n \times 2\pi\hbar/q$  leading to  $\theta = n\pi$  ( $n \in \mathbb{Z}$ ). We can understand Dirac’s argument as follows: since there is no well-defined winding number between two point particles in three dimensions, there can be no topological phase which restricts the charge of potential magnetic monopoles.

The general idea of how to use identical particles for topological quantum computation is the following. In the standard gate model of quantum computers, a calculation consists of three steps: (1) initialization in the state  $|i\rangle = |0, 0, \dots\rangle$ , (2) application of a gate  $U$  (a general unitary operator) on  $|i\rangle$  which produces  $|f\rangle = U|i\rangle$ , (3) measurement of the outcomes  $o_j \in \{0, 1\}$  in the computational basis with probabilities  $P(o_1, o_2, \dots) = |\langle o_1, o_2, \dots | f \rangle|^2$ . In a topological quantum computer, the three steps are replaced by operations involving anyons [7]: (1) the initialization is replaced by splitting a pair of anyons out of the vacuum, (2) a gate is done by *braiding* the anyons with each other, (3) the measurement is performed by fusion (pairwise annihilation), see Fig. 4(c).

<sup>1</sup>The transformation of a general parastatistics to bosons/fermions with potentially additional internal degrees of freedom is called the Klein transformations.

<sup>2</sup>The factor  $\frac{1}{2}$  arises as exchanging the particles only moves them halfway around each other.

To obtain nontrivial gates, braiding should perform a unitary gate on the ground state manifold. Since Abelian anyons only produce phases, they are not useful for this task but rather non-Abelian anyons are needed. Note that the computation on non-Abelian anyons is topological. The trajectories (worldlines) in the process splitting-braiding-fusion form a knot in space-time. The result of the computation does not depend on the concrete form of the worldlines but only on the topology of the knot. It is in this respect that the computation performed by non-Abelian anyons is robust.

The outline of the lecture is as follows: first, we will introduce the notion of a topological superconductor. Then, we will show that Majorana zero modes appear as zero energy solutions of the Bogoliubov-de Gennes equation describing a spinless  $p$ -wave superconductor in one dimension. The zero modes will turn out to be non-Abelian anyons called Ising anyons. However, note that braiding of Ising anyons does not result in the application of any arbitrary unitary gate. Thus, we will introduce an alternative class of anyons called ‘Fibonacci anyons’. We will show that they are in fact universal, i.e., an arbitrary computation can be performed by braiding. There are by now several reviews where further information on these subjects can be found. For Majorana zero modes, see for example Refs. [8–10]. More information about topological quantum computation can be found in Refs. [7, 11–14].

## 2 Topological superconductors

In the context of quantum mechanics, topology refers to a static system described by a Hamiltonian where the properties of certain eigenstates are insensitive to small perturbations (disorder). In order that these states are not affected by hybridization with other states of the system, the energy necessarily has to be in an energy gap (bandgap) of the system such that direct coupling is forbidden by energy conservation.

### 2.1 Topological quantum number

A prime example of a topological system in one dimension (1D) is given by the Jackiw-Rebbi (JR) model (1976) with the Hamiltonian [15]

$$H_{\text{JR}} = v_F p \sigma^z + M(x) \sigma^x = \begin{pmatrix} -i\hbar v_F \partial_x & M(x) \\ M(x) & i\hbar v_F \partial_x \end{pmatrix}, \quad (1)$$

where  $\sigma^j$  denote the Pauli matrices which represent an (artificial) spin degree of freedom. The first term describes the motion of a particle with velocity  $\pm v_F$  and momentum  $p = -i\hbar \partial_x$ . The particle is chiral as the direction ‘ $\pm$ ’ of motion depends on the spin. The second term proportional to  $M(x)$  leads to backscattering (as it couples the two directions of motion) and the appearance of a ‘mass’, i.e., a gap in the energy spectrum, see below.

Let us first discuss the case where the mass does not depend on position with  $M(x) \equiv \bar{M}$ . In this case, the system is translation-invariant and we can find eigenstates of the form

$$\psi_k = e^{ikx} \mathbf{v}_k. \quad (2)$$

Solving the eigenvalue equation  $H_{\text{JR}} \psi_k = E_k \psi_k$  in this case, leads to the result

$$E_k = \pm \sqrt{(\hbar v_F k)^2 + \bar{M}^2}, \quad \mathbf{v}_k = \begin{pmatrix} E_k - k \\ \bar{M} \end{pmatrix}. \quad (3)$$

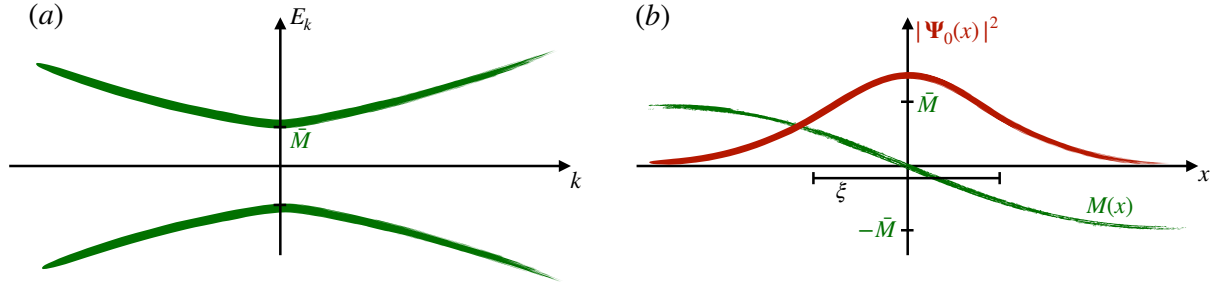


Figure 1: (a) Spectrum of the Jackiw-Rebbi model. It consists of two bands, one at positive and one at negative energies  $E_k$ . For large momentum  $\hbar k$ , the spectrum assumes the form  $E_k = \pm v_F \hbar |k|$ . Close to  $k \approx 0$ , there is an anticrossing with a bandgap of size  $2\bar{M}$ . (b) Probability distribution  $|\Psi_0(x)|^2$  for finding the particle in the bound state with  $E = 0$  at the position  $x$ . It is peaked at the position  $x \approx 0$  where the mass changes sign. The decay happens on the characteristic scale  $\xi = \hbar v_F / \bar{M}$ , which is proportional to the inverse gap.

Looking at the spectrum, cf. Fig. 1(a), we see that the JR Hamiltonian is a model for a 1D semiconductor with a bandgap of  $2|\bar{M}|$ . At first sight, it looks like the sign of  $\bar{M}$  does not matter.

However, let us see what happens if we bring a semiconductor with a positive bandgap  $\bar{M} > 0$  in proximity to a semiconductor with a negative bandgap  $-\bar{M}$ . We model this system by a mass  $M(x)$  that depends on position and assumes the asymptotic values  $M(x) \rightarrow \pm \bar{M}$  for  $x \rightarrow \mp \infty$ , see Fig. 1(b). We claim that, in this case, there will be a single state with energy  $E = 0$ . We show this by directly computing the eigenstate, i.e., solving the problem

$$H_{\text{JR}} \Psi_0 = -i \hbar v_F \sigma^z \partial_x \Psi_0 + M(x) \sigma^x \Psi_0 = 0. \quad (4)$$

After a slight rearrangement, using  $\sigma^z \sigma^x = i \sigma^y$ , we obtain

$$\frac{d}{dx} \Psi_0(x) = \kappa(x) \sigma^y \Psi_0(x), \quad \text{with} \quad \kappa(x) = \frac{M(x)}{\hbar v_F}, \quad (5)$$

with the solutions

$$\Psi_0 = \mathcal{N} \exp \left[ \pm \int_0^x dx' \kappa(x') \right] \chi_{\pm y}, \quad \chi_{\pm y} = \frac{1}{\sqrt{2}} \begin{pmatrix} e^{i\pi/4} \\ \pm e^{-i\pi/4} \end{pmatrix}, \quad (6)$$

where  $\mathcal{N} > 0$  is the normalization constant and  $\chi_{\pm y}$  denote the eigenvectors of  $\sigma^y$  to the eigenvalues  $\pm 1$ .

For our choice of  $M(x)$ , we have that

$$\int_0^x dx' \kappa(x') \rightarrow \mp \infty, \quad x \rightarrow \pm \infty. \quad (7)$$

In order for the state  $\Psi_0$  to be normalizable, we are only allowed to take the ‘+’ sign in Eq. (6). Concluding, we have found the bound eigenstate  $\Psi_0(x) \propto \exp \left[ \int_0^x dx' \kappa(x') \right] \chi_{+y}$  of the JR model at energy zero. The rest of the spectrum consists of extended states above the gap with energy  $|E| \geq \bar{M}$ . The energy of the state  $\Psi_0$  is within the gap.

Recapitulating the argument that has led to the identification of  $\Psi_0$ , we realize that the presence of the state is independent of the concrete form of  $M(x)$  and only depends on the sign of the asymptotic values for  $x \rightarrow \pm\infty$ . It is in this sense that the state  $\Psi_0$  is topological and is insensitive to disorder. In fact, one calls  $\mathcal{Q} = \text{sgn} M$  a  $(\mathbb{Z}_2)$  topological charge that can take values of  $\pm 1$ . When bringing two systems with opposite topological charges into proximity, a bound state within the gap is trapped at the interface. This state is insensitive to disorder because its presence is guaranteed by the properties (topological charge) of the bulk away from the interface.

## 2.2 Kitaev model

Kitaev (2001) introduced a Hamiltonian (called the Kitaev model) that implements the JR model in a one-dimensional (1D) superconducting system. The model is given by [16]

$$H_K = \sum_p \xi_p c_p^\dagger c_p + \frac{1}{2} \sum_p \Delta p (c_{-p} c_p + c_p^\dagger c_{-p}^\dagger), \quad (8)$$

where  $c_p$  are fermionic annihilation operators that obey the canonical anticommutation relation  $\{c_p, c_q^\dagger\} = \delta_{p,q}$ ,  $\{c_p, c_q\} = 0$ . The first term described spinless electrons with momentum  $p$  and energy  $\xi_p = p^2/2m - \mu$  relative to the chemical potential  $\mu$ . The second term proportional to  $\Delta > 0$  describes the superconducting pairing.<sup>3</sup> As we will see below, the fact that the problem is realized in a superconductor has crucial implications for the properties of the bound state  $\Psi_0$ . In fact, it turns out that the resulting excitations at the interface are Majorana zero modes that follow non-Abelian statistics useful for quantum computing.

In order to make contact with the JR model, we write the model in Nambu space

$$H_K = \frac{1}{2} \sum_p \mathbf{C}_p^\dagger H_{\text{BdG}}(p) \mathbf{C}_p \quad (9)$$

with  $\mathbf{C}_p = (c_p, c_{-p}^\dagger)^T$  and where we have introduced the Bogoliubov-de Gennes Hamiltonian

$$H_{\text{BdG}}(p) = \xi_p \tau^z + \Delta p \tau^x \quad (10)$$

with  $\tau^j$  the Pauli matrices acting on the Nambu space. Due to the fact that the Hamiltonian  $H_{\text{BdG}}$  is derived from  $H_K$  by doubling the degrees of freedom when going over from  $c_p$  to  $\mathbf{C}_p$ , it enjoys the relation  $\tau^x H_{\text{BdG}}(-p) \tau^x = -H_{\text{BdG}}(p)$ . As a result, each eigenmode of  $H_K$  leads to two eigenstates: for each eigenstate  $\Psi_E(p)$  of  $H_{\text{BdG}}$  at energy  $E$ , there is a state  $\tau^x \Psi_E(-p)$  at energy  $-E$ .

As above, we are interested in states close to  $E = 0$ . The Hamiltonian  $H_{\text{BdG}}$  allows for such a state only when  $p = 0$  (such that the second term vanishes) and  $\mu = 0$  (such that the first term vanishes). To describe the physics near the band closing at  $\mu = 0$  and  $p = 0$ , we expand around  $p = 0$ :<sup>4</sup>

$$H_{\text{BdG}} \approx -\mu \tau^z + \Delta p \tau^x. \quad (11)$$

We see that  $H_{\text{BdG}}$  is, in fact, the JR model with the replacement

$$\sigma^z \mapsto \tau^x, \quad v_F \mapsto \Delta, \quad (12)$$

$$\sigma^x \mapsto -\tau^z, \quad M \mapsto \mu. \quad (13)$$

<sup>3</sup>The pairing is of  $p$ -type because there is no  $s$ -wave pairing for spinless electrons.

<sup>4</sup>Treating the rest as a perturbation that can be included in principle later on.

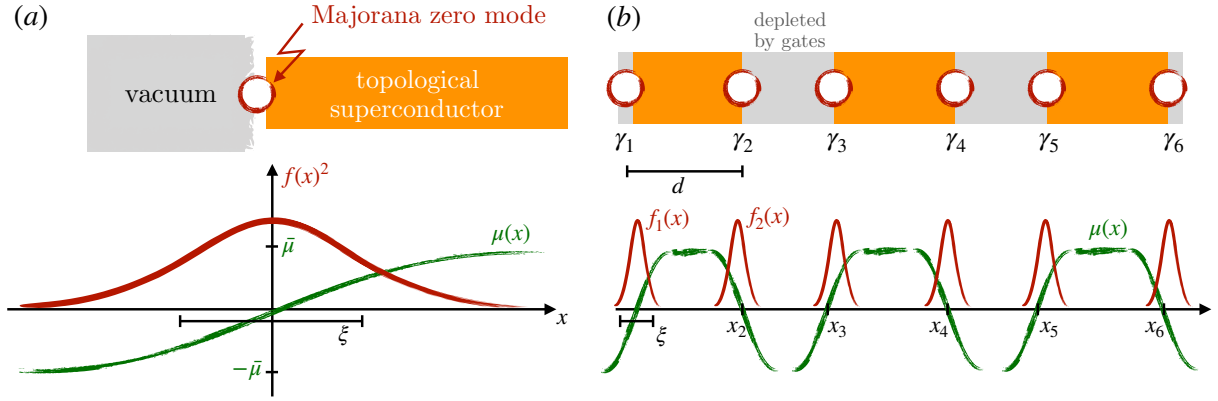


Figure 2: (a) A Majorana zero mode appears at the interface between a 1D topological superconductor and the vacuum. The vacuum is modeled by a negative chemical potential  $\mu$  such that there are no electrons present. (b) Segments of a topological superconductor can be depleted by gates. In our effective model, the gates lead to a negative chemical potential. At each domain wall (interface between the ‘vacuum’ and the superconductor) at position  $x_j$  a Majorana zero mode emerges. Due to the overlap proportional to  $\exp(-d/\xi)$  with  $\xi = \hbar\Delta/\bar{\mu}$ , these modes are not exactly at zero energy but at an energy  $\epsilon \simeq \bar{\mu}e^{-d/\xi}$ .

With that, we can identify the sign of  $\mu$  with the topological charge. Indeed, the Kitaev model  $H_K$  describes a topological superconductor when  $\mu > 0$ . For  $\mu < 0$ , the electrons are depleted from the wire, and the state is a conventional insulator.

The mapping of  $H_{\text{BdG}}$  onto the JR-model allows us to predict that an end state will appear at the interface of a topological superconductor ( $\mu > 0$ ) to vacuum ( $\mu < 0$ ). In particular, we model the situation in Fig. 2 by a chemical potential  $\mu(x)$  that changes sign at  $x = 0$ . The Hamiltonian  $H_{\text{BdG}}$  has the bound state

$$\Psi_0(x) = f(x)\chi_{+y}, \quad f(x) = \mathcal{N} \exp\left[\int_0^x dx' \mu(x')/\hbar\Delta\right] \quad (14)$$

at energy  $E = 0$ , which is localized close to the interface at  $x = 0$ . It is separated by a gap  $\bar{\mu}$  from the extended states.

### 2.3 Majorana zero modes

As we have seen before, a single eigenmode of  $H_K$  with energy  $E > 0$  corresponds to two states of  $H_{\text{BdG}}$  with energy  $\pm E$ . It is thus interesting to understand what the single state of  $H_{\text{BdG}}$  at  $E = 0$  corresponds to. To this end, we calculate the second-quantized operator

$$\gamma = \sqrt{2} \sum_p \int dx \Psi_0(x)^* \cdot \mathbf{C}_p e^{ipx/\hbar} = \int dx f(x) \left[ e^{i\pi/4} \psi(x) + e^{-i\pi/4} \psi^\dagger(x) \right] \quad (15)$$

that corresponds to the eigenstate  $\Psi_0$ ; here,  $\psi(x) = \sum_p e^{ipx/\hbar} c_p$  is the field operator that annihilates a particle at the position  $x$  and fulfills the anticommutation relations  $\{\psi(x), \psi^\dagger(x')\} = \delta(x - x')$ ,  $\{\psi(x), \psi(x')\} = 0$ .

The fermionic mode  $\gamma$  is special in that it is Hermitian with  $\gamma^\dagger = \gamma$ . In physical terms, this means that annihilating an excitation in the mode  $\gamma$  is the same as creating one. Such an excitation is only possible at zero energy which corresponds to the chemical potential of the superconductor. Due to the aforementioned Hermiticity, the excitation described by  $\gamma$  is called *Majorana zero mode*. With a straightforward calculation, one can show that  $\gamma^2 = \gamma^\dagger\gamma = 1$ . Generalizing these properties to multiple points  $x_j$  where the chemical potential  $\mu$  changes sign, we obtain a Majorana zero mode  $\gamma_j$  at each interface (domain wall) at  $x_j$ . These modes fulfill the Clifford algebra

$$\{\gamma_i, \gamma_j\} = 2\delta_{i,j} \quad (16)$$

which encodes the normalization  $\gamma_j^2 = 1$  together with the fermionic statistics  $\gamma_i\gamma_j = -\gamma_j\gamma_i$ .

As we have seen before, a single Majorana zero mode  $\gamma$  that is pinned at the position where the chemical potential changes sign is pinned at zero energy. We can understand this in algebraic terms by noting that the effective low energy Hamiltonian  $H_{\text{eff}}$  can only involve the excitation  $\gamma$  as the other excitations are at the energy  $\bar{\mu}$ . Due to superselection (see below), each term of a Hamiltonian has to involve an even power of fermionic operators. However, all such terms are trivial as  $\gamma^{2n} = (\gamma^2)^n = 1$  so the effective Hamiltonian vanishes.

This argument does not work any more as soon as two Majorana zero modes  $\gamma_1$  and  $\gamma_2$  are present. In fact, there is only one Hermitian combination  $i\gamma_1\gamma_2$  that involves an even number of fermionic operators. So the effective Hamiltonian has to be of the form

$$H_{\text{eff}} = \epsilon i\gamma_1\gamma_2. \quad (17)$$

In fact, the energy  $\epsilon$  is approximately given by the overlap

$$\epsilon \approx \langle f_1 | H_{\text{BdG}} | f_2 \rangle \simeq \bar{\mu} \int dx f(x - x_1)^* f(x - x_2) \simeq \bar{\mu} e^{-d/\xi} \quad (18)$$

with  $d = |x_2 - x_1|$ , the distance between the zero modes, and  $\xi = \hbar\Delta/\bar{\mu}$ , the decay length that is proportional to the inverse gap.

### 3 Majorana qubits

We have seen that the low energy properties of a topological superconductor are given by the Majorana zero modes  $\gamma_j$  that are pinned at the domain walls where the sign of  $\mu$  changes. We are interested in the Hilbert space that can be accessed by acting with the modes  $\gamma_j$  on the ground state  $|0\rangle$ . It is an easy exercise in algebra to show that given a set of  $2N$  Majorana zero modes, we can construct  $N$  Dirac fermions  $c_j$  via

$$c_j = \frac{1}{2}(\gamma_{2j-1} + i\gamma_{2j}), \quad c_j^\dagger = \frac{1}{2}(\gamma_{2j-1} - i\gamma_{2j}). \quad (19)$$

The Dirac fermions fulfill the canonical anticommutation relations  $\{c_i, c_j^\dagger\} = \delta_{i,j}$  and  $\{c_i, c_j\} = 0$ .

The Hilbert space of a single fermionic mode ( $N = 1$ ) is two-dimensional: the mode is either filled or empty, distinguished by the eigenvalue of the number operators  $n_j = c_j^\dagger c_j$  which have eigenvalues 0 or 1.<sup>5</sup> Operators that will turn out to be important in the following

<sup>5</sup>Note that  $n_j$  is idempotent as  $n_j^2 = c_j^\dagger c_j c_j^\dagger c_j = c_j^\dagger (1 - c_j^\dagger c_j) c_j = n_j$ , which proves that the eigenvalues of  $n_j$  are 0 or 1.



discussion are the fermion parity operators  $\mathcal{P}_j = 1 - 2n_j = (-1)^{n_j}$ , which have the eigenvalue  $+1$  if the number of fermions is even and  $-1$  if the number of fermions is odd. In terms of the Majorana operators, the parity operators assume the simple form

$$\mathcal{P}_j = -i\gamma_{2j-1}\gamma_{2j}. \quad (20)$$

If we think about an implementation for a quantum computer, we are used to the example of a spin- $\frac{1}{2}$  particle which is a model system for a generic two-level system [17]. However, we can ask ourselves the question whether we can also use the many-body Fock space for quantum computation purposes. We know that the occupation states  $|n_1, n_2, \dots, n_N\rangle$  with  $n_j \in \{0, 1\}$  form a basis for the  $N$ -mode fermionic Fock space generated by the creation operators  $c_j^\dagger$ ,  $j \in \{1, \dots, N\}$ , starting from the vacuum state denoted by  $|0\rangle$ . The Fock space has dimension  $2^N$  (each mode can be either occupied or empty). Thus counting the degrees of freedom, we are tempted to conclude that a fermionic system with  $N$  modes emulates  $N$  qubits. In the next section, we will see that this naïve counting argument is not completely correct as it violates the so-called superselection rule.

### 3.1 Fermionic quantum computation

Expressing a Hamiltonian  $H$  or in fact any physical observable  $A$  which are bosonic operators in terms of fermionic creation and annihilation operators, we are bound to only include terms where an even number of fermion operators appear.<sup>6</sup> The result is that the total fermion parity  $\mathcal{P} = \prod_j \mathcal{P}_j = (-1)^{\sum_j n_j}$  is strictly conserved in a closed system; the reason for this is the fact that

$$\mathcal{P}A\mathcal{P} = A \quad (21)$$

which follows from  $\mathcal{P}c_j\mathcal{P} = -c_j$  and the fact that each term in  $A$  involves an even number of fermionic operators. Note that the superconducting Hamiltonian (8) conserves the total fermion parity even so the number of fermions is not conserved. Due to this constraint, we have the following superselection rule: given two states in a fermionic Fock space  $|\psi_+\rangle$  and  $|\psi_-\rangle$  with different fermion parity,  $\mathcal{P}|\psi_\pm\rangle = \pm|\psi_\pm\rangle$  we have

$$\langle\psi_-|A|\psi_+\rangle = \langle\psi_-|\mathcal{P}A\mathcal{P}|\psi_+\rangle = -\langle\psi_-|A|\psi_+\rangle = 0 \quad (22)$$

for all observables  $A$ . Thus, there is no point in making superpositions between states of different parity as there will be no effect on any observable. We can restrict ourselves to one superselection sector and keep the total fermion parity fixed with either  $\mathcal{P} = +1$  or  $\mathcal{P} = -1$ . The conclusion of this argument is that out of the  $2^N$  states in a fermionic Fock space, only  $2^{N-1}$  can be effectively used for quantum computation purposes.

A further restriction to quantum computation using fermions arises from the fact that noninteracting fermions subject to beam splitters, phase-shifters (delay lines), measurements of the state of a single electron (so-called fermionic linear optics) does not in fact lead to any entanglement [18]. In order to generate entanglement, we need to add parity measurement of two electrons which effectively involves interactions between different electrons [19, 20].

---

<sup>6</sup>From the correspondence principle, we know that for large quantum numbers the expectation values of operators for physical observables should behave like (real) numbers. Due to the anticommutation relation of fermionic operators, the correspondence principle for a potential fermionic observable would instead lead to anticommuting Grassmann numbers on the classical level.



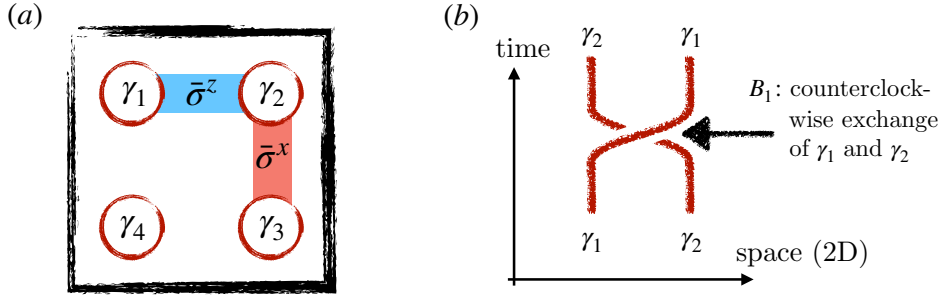


Figure 3: (a) Sketch of the parity Majorana qubit: Two Majorana zero modes together form a single Dirac fermionic mode whose Hilbert space is two-dimensional as the mode can either be empty or filled. Both states have the same energy. Four Majorana zero modes thus form a four-dimensional Hilbert space of which, due to the conservation of the total fermion parity, only a two-dimensional subspace can be accessed. This degenerate, two-dimensional subspace is the Majorana qubit. Gates on the qubit can be performed either by braiding or by coupling two Majorana zero modes. As indicated in the figure, coupling  $\gamma_1$  to  $\gamma_2$  implements a  $\bar{\sigma}^z$ -operation, whereas coupling  $\gamma_2$  to  $\gamma_3$  leads to a  $\bar{\sigma}^x$ -operation. Given the fact that the Majorana zero modes are sufficiently far apart from each other and that the environment only acts locally on the system, these operations are not performed ‘accidentally’ by the environment and the Majorana qubit is protected from both sign flip and bit flip errors. As this protection originates from the conservation of the total fermion parity, the qubit is called parity-protected. (b) Elementary operation of the braid group. The geometric representation of the braid group is in space-time; the horizontal axis is the spatial axis whereas the vertical one is temporal. The counterclockwise exchange of Majorana zero modes  $\gamma_1$  and  $\gamma_2$  in space-time forms the braid  $B_1$ .

### 3.2 Encoding of a qubit

We have seen in the last section that due to the parity-conservation, we need to have two fermionic modes to encode a single qubit. For concreteness, we will work in the even parity superselection sector and have the single logical qubit encoded as  $|\bar{0}\rangle = |00\rangle$  and  $|\bar{1}\rangle = |11\rangle$ . Thinking about a possible implementation in terms of Majorana modes, we encode each fermionic mode in a pair of Majorana zero modes which are localized states sufficiently far separated from each other, see Fig. 3. We denote the Majorana zero modes on the top as  $\gamma_1$  and  $\gamma_2$ , and the ones on the bottom as  $\gamma_3$  and  $\gamma_4$ . The Majorana modes are at zero energy thus the two states  $|\bar{0}\rangle$  and  $|\bar{1}\rangle$  are degenerate in energy. The parities of the number of electrons on the superconducting segments are given by  $\mathcal{P}_1 = -i\gamma_1\gamma_2$  and  $\mathcal{P}_2 = -i\gamma_3\gamma_4$ . Due to the parity constraint, we have  $\mathcal{P}_1 = \mathcal{P}_2$  and the action of both operators on the logical qubit emulates the (logical) Pauli-operator

$$\bar{\sigma}^z = -i\gamma_1\gamma_2 = -i\gamma_3\gamma_4. \quad (23)$$

In order to have a complete qubit, we are left with the task of finding a logical  $\bar{\sigma}^x$ , an operator which anticommutes with  $\bar{\sigma}^z$ . It is easy to see that

$$\bar{\sigma}^x = -i\gamma_2\gamma_3 = -i\gamma_1\gamma_4 \quad (24)$$

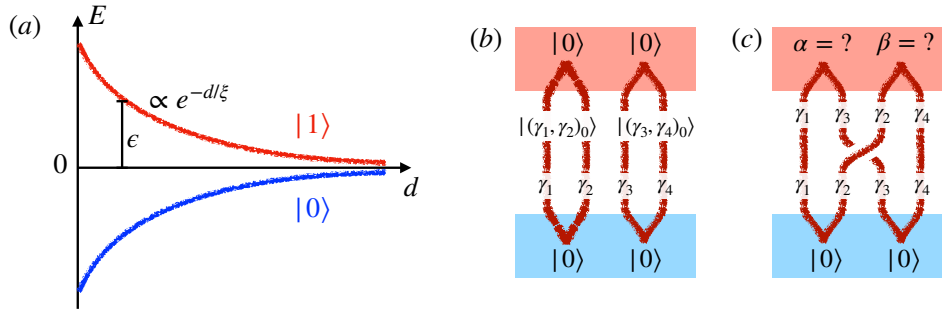


Figure 4: (a) Bringing two Majorana zero modes in close proximity (called fusion) such that their distance  $d$  is of the decay length  $\xi$ , the energy difference  $\propto \exp(-d/\xi)$  between the state  $|0\rangle$  and  $|1\rangle$  breaks the parity protection. By measuring whether or not the system is in the ground state, a projective measurement in the computational basis states  $|0\rangle$  and  $|1\rangle$  is performed. Similarly, we can split the Majorana zero modes that are initialized in the ground state  $|0\rangle$  and produce a parity protected state. (b) The fusion outcome (red box) of Majorana zero modes that have been initialized to the vacuum (by splitting, blue box) is well-defined. (c) If the Majorana zero modes have been interchanged (braided), the fusion outcomes  $\alpha, \beta$  fluctuate.

anticommutes with  $\bar{\sigma}^z$  due to the fact that the single Majorana fermions shared by both operators anticommute with one another. In the situation where all the Majorana modes are sufficiently far separated from each other, any gate on the logical qubit is a nonlocal operator. Due to this nonlocality, it is highly unlikely that uncontrolled, random fluctuations in the environment will execute a gate and thus cause an error on the logical qubit. This protection of the Majorana qubit is called symmetry-protected topological order [21, 22] or simply parity-protection [23]. The decisive difference to full topological order, as it is for example present in Kitaev's toric code [24], is the fact that logical Pauli operators are only required to be nonlocal as long as the parity symmetry is conserved. A tunneling of single electrons from a reservoir onto the superconducting island is a local process that violates parity conservation, immediately bringing the Majorana qubit out of its computational subspace.

The requirement for operating the Majorana qubit successfully in a protected manner is that the environment does not provide single unpaired electrons. This sounds very stringent at first sight. However, the physical implementation of the system only involves superconductors where most of the electrons are paired up into Cooper pairs and where, at temperature  $T$ , only an exponentially small fraction proportional to the Boltzmann factor  $e^{-\Delta/k_B T}$  remains unpaired. The storage time of quantum information in a Majorana qubit thus is expected to increase exponentially when lowering the electron temperature.

### 3.3 Fusion and splitting

We have seen before that if you bring the Majorana zero modes  $\gamma_1$  and  $\gamma_2$  close together, there is a finite energy splitting  $\epsilon \simeq \bar{\mu}e^{-d/\xi}$  due to the overlap of the modes, see Fig. 4(a). This splitting breaks the parity protection and as a result the two states  $|0\rangle$  and  $|1\rangle$  are no longer degenerate in energy. It is then possible to detect in which state the system is [12, 23, 25]. The process of bringing two Majorana modes together is called fusion. Graphically, we

denote the fusion experiment as the red box in Fig. 4(b). The fusion experiment implements the measurement in the computational basis and is the last step in a quantum computation.

The reverse process is called splitting and is depicted as the blue box in Fig. 4(b). If one starts with the vacuum state  $|0\rangle$  when the Majorana zero modes are overlapping, the Majorana states can be separated from each other such that the initial state  $|0\rangle$  becomes degenerate with  $|1\rangle$  and parity protection is achieved. It is clear that if one fuses the zero modes again immediately after the splitting, the outcome of the fusion experiment is the state  $|0\rangle$  with certainty, see Fig. 4(b). On the other hand, if the pairing is changed such that at the fusion different Majorana zero modes are paired up as in the splitting, the result is unclear, see Fig. 4(c).

As we are now thinking about different ways of pairing the Majorana zero modes to produce a Dirac fermion that can be either empty or occupied, it is useful to introduce the notation  $|(\gamma_1, \gamma_2)_j\rangle$ . It denotes whether the state formed by  $\gamma_1$  and  $\gamma_2$  is occupied ( $j = 1$ ) or empty ( $j = 0$ ). With this new notation, we can write for the logical states

$$|\bar{0}\rangle = |(\gamma_1, \gamma_2)_0 (\gamma_3, \gamma_4)_0\rangle, \quad |\bar{1}\rangle = |(\gamma_1, \gamma_2)_1 (\gamma_3, \gamma_4)_1\rangle. \quad (25)$$

The fusion experiment in Fig. 4(c) produces the outcome  $\alpha, \beta \in \{0, 1\}$  with probability

$$P(\alpha, \beta) = \left| \langle (\gamma_1, \gamma_3)_\alpha (\gamma_2, \gamma_4)_\beta | (\gamma_1, \gamma_2)_0 (\gamma_3, \gamma_4)_0 \rangle \right|^2. \quad (26)$$

Due to the conservation of total parity  $\mathcal{P}$ , the only possible outcomes are  $\alpha = \beta = 0$  and  $\alpha = \beta = 1$ . We will calculate the probabilities in the next section. However, we must first introduce the part of Fig. 4(c) in between the splitting and the fusion of the Majorana zero modes. The exchange of the zero modes is called braiding.

## 4 Braiding

Exchange statistics is introduced in the basic physics courses as the action of permutations of the symmetric group  $\mathcal{S}_N$  with  $N!$  elements on the wavefunction of  $N$  identical particles. There are two possibilities: either the wavefunction remains invariant (‘bosons’) or the wavefunction acquires a minus sign (‘fermions’) under the exchange of two particles. On a mathematical level, the origin of this distinction lies in the fact that the Hamiltonian of identical particles commutes with an arbitrary element of the symmetric group  $\mathcal{S}_N$ . Thus, it is possible to classify the eigenstates of the Hamiltonian in terms of irreducible representations of the permutation group. There are only two one-dimensional representations: the trivial representation (corresponding to bosons) and the sign representation (corresponding to fermions). Any representation whose dimension is larger than one leads to a degeneracy, which is called exchange degeneracy as it originates simply from the fact that particles are indistinguishable.<sup>7</sup> In fact, the spin-statistics theorem can be proven in the context of relativistic field theory in  $3 + 1$  dimensions, which states that particles with integer spin are bosons whereas particles with half-integer spin are fermions.

<sup>7</sup>The statistics of identical particles that transforms according to higher dimension representations of the permutation groups is called parastatistics. However, even if particles with parastatistics were to exist, they would offer nothing new as a set of Klein transformations could be used to map particles with parastatistics onto bosons or fermions with a set of internal quantum numbers (like spin, ...). Later, we will see that such a mapping is not possible in  $2 + 1$  dimensions and that higher dimensional representations of the braid group is truly different from the one-dimensional representations.

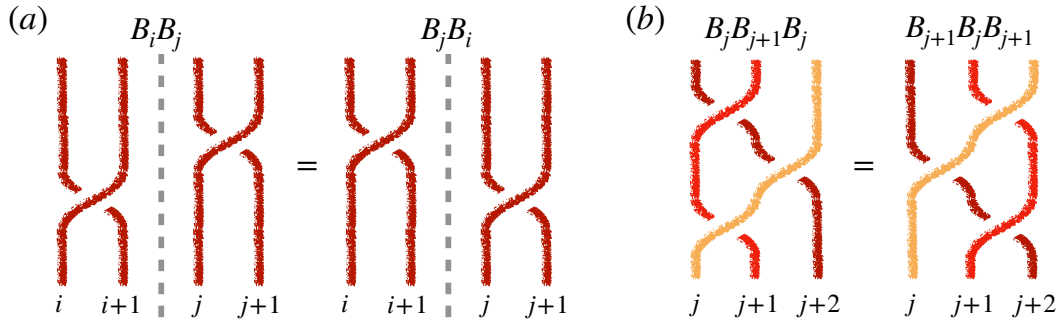


Figure 5: (a) Braiding operators commute if their index  $i$  and  $j$  are more than 2 apart. The reason is that  $B_i$  and  $B_j$  do not have any strand in common so either one can be executed first. (b) The Yang-Baxter equation  $B_j B_{j+1} B_j = B_{j+1} B_j B_{j+1}$  provides a nontrivial relation between the generators  $B_j$  and  $B_{j+1}$ . That the two braids are topologically equivalent can be seen as follows: in both braids the dark strand can be considered to lie in the very back and connects the initial position  $j+2$  to the final position  $j$ . Similarly, the bright strand lies in front and connects  $j$  to  $j+2$ . The middle strand starts at  $j+1$  and ends at the same place. The braids are equivalent as they can be deformed into each other by sliding the middle strand  $j+1$  in between the two other strands from the left to the right.

It has been pointed out that the physical process of exchanging two particles is important. In fact, the exchange of two identical particles has to be viewed as a (slow) process that occurs in space-time [26]. In  $2+1$  dimensions, the relevant group is the braid group  $\mathcal{B}_N$  of  $N$  strands as trajectories in space-time for exchanging two particles clockwise or counterclockwise are topologically distinct. The braid group  $\mathcal{B}_N$  consists of  $N$  strands. The generators of the group  $B_j$  denote the braiding strand  $j$  and  $j+1$  in the counterclockwise direction (in Fig. 3(b),  $B_1$  braids strand 1 and 2 counterclockwise). The inverse operation braids the strands clockwise. Two elements of the group are equivalent if the corresponding braids can be smoothly deformed into each other by keeping their ends fixed. Note that different from the symmetric group  $B_j \neq B_j^{-1}$ . The braid group of  $N$  strands is generated by  $B_1, \dots, B_{N-1}$  where the generators satisfy the following two relations (Artin [27]),

$$B_i B_j = B_j B_i, \quad |i - j| \geq 2 \quad \text{and} \quad B_j B_{j+1} B_j = B_{j+1} B_j B_{j+1}; \quad (27)$$

the latter is also called Yang-Baxter equation, see Fig. 5. Unlike the symmetric group  $\mathcal{S}_N$  the group order is infinity which makes the classification of all irreducible representations difficult.

In  $3+1$  dimensions, clockwise and counterclockwise depends on the observer (coordinate system) and thus the exchanges  $B_j$  and  $B_j^{-1}$  are topologically equivalent. As a result, we obtain  $B_j^2 = B_j^{-1} B_j = 1$ . Under this additional constraint, the braid group  $\mathcal{B}_N$  reduces to the symmetric group  $\mathcal{S}_N$ . The dependence of the exchange statistic on the dimension of space is as follows:

- 1D: no exchange of particles is possible
- 2D: the exchange is described by the braid group  $\mathcal{B}_N$

- 3D: we have  $B_j^2 = 1$  and the symmetric group  $\mathcal{S}_N$  characterizes the exchange (only bosons and fermions are possible)

We see that 2D is special. Thus, we will study some examples of nontrivial exchange statistics in 2 + 1 dimensions in the following.

## 4.1 Abelian anyons

The one-dimensional (unitary) representations of the braid group are simple to construct. In general, the action of  $B_j$  onto a wavefunction is given by a phase factor  $\rho(B_j) = e^{i\theta_j}$  with  $\theta_j \in [0, 2\pi)$ . The Yang-Baxter equation demands

$$\rho(B_j)\rho(B_{j+1})\rho(B_j) = \rho(B_{j+1})\rho(B_j)\rho(B_{j+1}) \Rightarrow e^{2i\theta_j+i\theta_{j+1}} = e^{i\theta_j+2i\theta_{j+1}} \Rightarrow \theta_j = \theta_{j+1}$$

for any 1D representation. As a result, all the angles are equal and the representation

$$\rho_\theta(B_j) = e^{i\theta} \quad (28)$$

is characterized by a single angle  $\theta$ .

Note that for  $\theta = 0$ , we get the customary result for bosons that interchanging two particles does nothing to the wavefunction whereas for  $\theta = \pi$  interchanging introduces a minus sign which is the result for fermions. In 2 + 1 dimensions, all angles in between 0 and  $\pi$  are allowed and particles with  $\theta \neq 0$  or  $\pi$  are called (Abelian) anyons. As an example, we note that quasiparticles in the fractional quantum Hall effect at filling fraction  $\nu = \frac{1}{n}$  with  $n$  an odd integer are anyons with  $\theta = \nu\pi$ . Even though the Abelian anyons are interesting from a physical point of view, they do not offer any resources that can be used for quantum computing as braiding only introduces simple phase factors.

Particles whose wavefunctions transform according to higher dimensional irreducible representations of the braid group are called non-Abelian anyons. A necessary ingredient is a ground state degeneracy (which grows exponentially with the number of particles). The effect of  $B_j$ , the counterclockwise exchange of two particles  $j$  and  $j + 1$ , is then represented by a unitary matrix  $\rho(B_j)$  on the ground state manifold. As different unitary matrices do not commute, the representation is non-Abelian which is the reason for their name.

The usefulness of non-Abelian anyons for topological quantum computation relies on the fact that the degeneracy of the ground state manifold is protected, and the gates implemented by the exchange of particles are exact (up to an unimportant global phase) [12]. A specific species of non-Abelian anyons is called universal for quantum computation, if, for any given gate, a braid can be found which approximates the gate with arbitrary accuracy.

## 4.2 Ising anyons

We have seen that Majorana zero modes in topological superconductors lead to a degenerate ground state of size  $2^{N-1}$  that grows exponentially with the number of zero modes. It is thus a natural question to ask if the process of braiding the zero modes lead to a nontrivial operation  $\rho_\gamma(B_j)$  on the ground state manifold. It can be shown, see the Appendix, that braiding of Majorana zero modes in topological superconductors is described by the unitary representation [28–32]

$$\rho_\gamma(B_j) = \exp\left(-\frac{\pi}{4}\gamma_j\gamma_{j+1}\right) = \frac{1}{\sqrt{2}}(1 - \gamma_j\gamma_{j+1}) \quad (29)$$

of the braid group. The representation  $\rho_\gamma$  is also called Ising anyons. The clockwise exchange of the strands  $j$  and  $j+1$  is implemented by  $\rho_\gamma(B_j^{-1}) = \rho_\gamma(B_j)^\dagger = \rho_\gamma^\dagger(B_j) = \exp\left(\frac{\pi}{4}\gamma_j\gamma_{j+1}\right)$ .

Under the action of  $\rho_\gamma(B_j)$ , the Majorana zero modes are mapped onto each other with

$$\gamma'_j = \rho_\gamma^\dagger(B_j)\gamma_j\rho_\gamma(B_j) = -\gamma_{j+1}, \quad \gamma'_{j+1} = \rho_\gamma^\dagger(B_j)\gamma_{j+1}\rho_\gamma(B_j) = \gamma_j \quad (30)$$

while the other modes remain unaffected. That this is the correct expression is reinforced by the fact that the (local) parity

$$\mathcal{P}'_j = \rho_\gamma^\dagger(B_j)\mathcal{P}_j\rho_\gamma(B_j) = -i\gamma'_j\gamma'_{j+1} = -i\gamma_j\gamma_{j+1} = \mathcal{P}_j \quad (31)$$

is conserved [33].

To check that  $\rho_\gamma$  is a representation of the braid group, we have to check  $\rho_\gamma(B_i)\rho_\gamma(B_j) = \rho_\gamma(B_j)\rho_\gamma(B_i)$ ,  $|i-j| \geq 2$ , and the Yang-Baxter equation, see Eq. (27). The first relation follows easily as  $\rho_\gamma(B_i)$  and  $\rho_\gamma(B_j)$  commute due to the fact that they act on different Majorana zero modes and consist of an even number of Majorana operators. The Yang-Baxter equation can be directly evaluated

$$\begin{aligned} \rho_\gamma(B_j)\rho_\gamma(B_{j+1})\rho_\gamma(B_j) &= \frac{1}{2^{3/2}}(1-\gamma_j\gamma_{j+1})(1-\gamma_{j+1}\gamma_{j+2})(1-\gamma_j\gamma_{j+1}) \\ &= -\frac{1}{\sqrt{2}}(\gamma_j\gamma_{j+1} + \gamma_{j+1}\gamma_{j+2}), \end{aligned} \quad (32)$$

and similarly

$$\rho_\gamma(B_{j+1})\rho_\gamma(B_j)\rho_\gamma(B_{j+1}) = -\frac{1}{\sqrt{2}}(\gamma_j\gamma_{j+1} + \gamma_{j+1}\gamma_{j+2}); \quad (33)$$

as a result, the unitary gate performed by braiding Majorana zero modes only depends on the braid and not on the specific paths taken. In particular, both methods depicted in Fig. 5(b) of moving the Majorana zero modes around each other produces the same operation on the ground state manifold.

Thus, braiding can be used to perform topologically protected gates onto the encoded Majorana qubit states  $|\bar{0}\rangle$  and  $|\bar{1}\rangle$ . Indeed, for  $N=4$ , the interchange of Majorana zero modes implements the operations

$$\rho_\gamma(B_1) = \rho_\gamma(B_3) = \exp\left(-i\frac{\pi}{4}\bar{\sigma}^z\right), \quad \rho_\gamma(B_2) = \exp\left(-i\frac{\pi}{4}\bar{\sigma}^x\right) = \frac{1}{\sqrt{2}}(1-i\bar{\sigma}^x) \quad (34)$$

that correspond to rotations by  $90^\circ$  on the Bloch sphere.

We now have all the ingredients to calculate the probability  $P(\alpha, \beta)$  of Eq. (26), see Fig. 4(c). Performing the braid  $B_2$  acts as  $\rho_\gamma(B_2) = 2^{-1/2}(1-i\bar{\sigma}^x)$  on the ground state manifold. In particular, the initial state  $|\bar{0}\rangle = |(\gamma_1, \gamma_2)_0 (\gamma_3, \gamma_4)_0\rangle$  gets transformed into

$$\rho_\gamma(B_2)|\bar{0}\rangle = \frac{1}{\sqrt{2}}(|\bar{0}\rangle - i|\bar{1}\rangle) = \frac{1}{\sqrt{2}}(|00\rangle - i|11\rangle). \quad (35)$$

The probabilities  $P(\alpha, \beta)$  for the outcomes  $\alpha = \beta \in \{0, 1\}$  after the braid are given by

$$P(0, 0) = |\langle 00|\rho_\gamma(B_2)|\bar{0}\rangle|^2 = \frac{1}{2}, \quad P(1, 1) = |\langle 11|\rho_\gamma(B_2)|\bar{0}\rangle|^2 = \frac{1}{2}. \quad (36)$$



As the result  $P(\alpha, \alpha) = 50\%$  for both  $\alpha = 0$  and  $\alpha = 1$  originates from the representation of the braid group of the Majorana zero modes, the fusion experiment in Fig. 4(c) has been proposed recently as a first test of the non-Abelian nature of Majorana zero modes [34].

Even though these operations are protected, braiding of Ising anyons is not enough to perform arbitrary unitary operations on the ground state manifold. The single qubit rotations are not complete as only rotations by (multiples of)  $90^\circ$  around the coordinate axes  $x, y, z$  can be implemented. In particular, a rotation by  $45^\circ$  is missing (called  $\frac{\pi}{8}$ -phase or T-gate) and an entangling gate needs to be added [12, 35]. In concrete realizations, entanglement can be obtained by performing a joint parity measurement of two qubits [20, 23]. In fact, it is enough if the T-gate is implemented with a fidelity of 90% as a distillation protocol using the exact Clifford gates in a process called *Magic state distillation* can be employed to purify the state [35].

### 4.3 Fibonacci anyons

The Ising anyons provided by the Majorana modes have the nice property that they allow for noise-insensitive operations on a parity-protected qubit by braiding. Still, the group of operations that can be obtained in this way is not enough for universal quantum computation. However, luckily, there exist other anyons, in particular Fibonacci anyons, that allow for a universal set of operations by braiding [4, 12]. That Majorana zero modes do not offer universality is connected to the fact that the Hilbert space can be locally assigned to Majorana modes: any pair of Majorana zero modes can either be filled or empty. For Fibonacci anyons the relation between the anyons and the Hilbert space of the ground state thus has to be more complicated to overcome this issue.

We denote Fibonacci anyons with the letter  $\tau$ . A pair of Fibonacci anyons has two possible fusion outcomes: it can either fuse to the vacuum 0 or to a Fibonacci anyon  $\tau$ . In particular, we have that  $|(\tau_1, \tau_2)_0\rangle, |(\tau_1, \tau_2)_\tau\rangle$  forms a basis of the two-dimensional ground state manifold of two Fibonacci anyons. However, akin to the Ising anyons, there is a superselection rule forbidding us to use these two states as a qubit. The ‘Fibonacci qubit’ thus has to be formed from a subspace of three Fibonacci anyons  $\tau_1, \tau_2, \tau_3$  with the possible fusion outcomes<sup>8</sup>

$$|\bar{0}\rangle = |((\tau_1, \tau_2)_0, \tau_3)_\tau\rangle, \quad |\text{nc}\rangle = |((\tau_1, \tau_2)_\tau, \tau_3)_0\rangle, \quad |\bar{1}\rangle = |((\tau_1, \tau_2)_\tau, \tau_3)_\tau\rangle. \quad (37)$$

Note that the first and the last state are in the same superselection sector (as they fuse to  $\tau$ ) and thus can be used as a genuine Fibonacci qubit. The state of the qubit is then determined by the fusion outcome of the first two Fibonacci anyons while the fusion with the last Fibonacci anyon is constrained to be  $\tau$ . The third state with total fusion outcome 0 is then a noncomputational (nc) state.

For the Hilbert space of the degenerate ground state of the  $N$ -Fibonacci anyons  $\tau_1, \dots, \tau_N$ , we introduce the following notation

$$|0, \tau, f_2, \dots, f_N\rangle = |(\dots((\tau_1, \tau_2)_{f_2}, \tau_3)_{f_3}, \dots)_{f_N})\rangle, \quad f_j \in \{0, \tau\}, \quad (38)$$

where we have added the fusion outcomes 0 and  $\tau$  of the zeroth and first Fibonacci anyons for future convenience.

<sup>8</sup>Note that the fusion of the vacuum 0 with  $\tau$  can only give  $\tau$ .



	$ i\rangle =  f_{j-1}, f_j, f_{j+1}\rangle$	$\rho_\tau(B_j) i\rangle = \sum_{f'_j} c_{f'_j}  f_{j-1}, f'_j, f_{j+1}\rangle$
	$ 0, \tau, \tau\rangle$	$\omega^{-1} 0, \tau, \tau\rangle$
	$ \tau, \tau, 0\rangle$	$\omega^{-1} \tau, \tau, 0\rangle$
	$ 0, \tau, 0\rangle$	$\omega^{-2} 0, \tau, 0\rangle$
	$ \tau, 0, \tau\rangle$	$\phi^{-1}\omega^2 \tau, 0, \tau\rangle + \phi^{-1/2}\omega \tau, \tau, \tau\rangle$
	$ \tau, \tau, \tau\rangle$	$\phi^{-1/2}\omega \tau, 0, \tau\rangle - \phi^{-1} \tau, \tau, \tau\rangle$

Table 1: Result of the elementary braid  $B_j$  of Fibonacci anyons on the basis formed by the fusion outcomes. Note that the effect of braiding the strands  $j$  and  $j+1$  is local in the sense that it only changes the fusion outcome  $f_j$ . The parameters are the phase  $\omega = -q = -e^{2\pi i/5}$  and the golden ratio  $\phi = (1 + \sqrt{5})/2 = q + \bar{q} + 1$ .

A particular state is then labeled by writing the fusion outcome  $f_j$  in between strand  $j$  and  $j+1$ . In order to determine the dimension of the ground state, we have to find the number of states of the form in Eq. (38). The fusion outcomes  $f_0 = 0, f_1, \dots, f_N$  are only constrained by the fact that the fusion of the vacuum  $f_j = 0$  (at step  $j$ ) with a Fibonacci anyon necessarily gives a Fibonacci anyon as the fusion outcome and thus  $f_{j+1} = \tau$ . Thus, we need to count the number of states  $|0, \tau, f_1, \dots, f_N\rangle$  without two 0s in a row. Denoting by  $Z_j$  ( $O_j$ ) the number of states with  $f_j = 0$  ( $f_j = 1$ ), we have to solve the recurrence relations

$$Z_{j+1} = O_j, \quad O_{j+1} = O_j + Z_j, \quad O_0 = 0, \quad Z_0 = 1, \quad (39)$$

with the result  $Z_{j+1} = O_j = F_j$ ,  $F_j$  being the  $j$ -th Fibonacci number. Note that this relation is the reason why the anyons are called Fibonacci anyons.

The unitary representation  $\rho_\tau(B_j)$  of braiding the Fibonacci anyons  $\tau_j$  and  $\tau_{j+1}$  can be expressed as a local relation of the fusion outcomes  $f_{j-1}, f_j, f_{j+1}$ , see Table 1 and [36, 37].<sup>9</sup> It can be directly checked that  $\rho_\tau$  is unitary. To check that it is, in fact, a representation, we have to prove Eq. (27). As before, the first relation in (27) follows from the fact that  $\rho_\tau(B_j)$  only depends on  $f_{j-1}, f_j, f_{j+1}$  and only changes the value of  $f_j$ . As a result,  $\rho(B_i)$  trivially commutes with  $\rho(B_j)$  for  $|i - j| \geq 2$ .

In the last step, we have to test whether  $\rho_\tau$  satisfies the Yang-Baxter equation. As for the Ising anyons, we do this directly by calculating  $UVU$  and  $VUV$  with  $U = \rho_\tau(B_j)$  and  $V = \rho_\tau(B_{j+1})$  separately and subsequently verify that  $UVU = VUV$ . The Yang-Baxter equation acts on the three strands  $j, j+1, j+2$ . In the first step, we determine the representation of  $\rho_\tau(B_j)$  and  $\rho(B_{j+1})$  in the Hilbert space  $|f_{j-1}, f_j, f_{j+1}, f_{j+2}\rangle$ . Note that we suppress the labels of the other fusion outcomes as they remain unchanged. Moreover, we see from Table 1 that  $U$  and  $V$  cannot change the value of  $f_{j-1}$  and  $f_{j+2}$  (superselection rule) and thus we can verify the relation for each value of  $a = f_{j-1}$  and  $b = f_{j+2}$  separately.

With the rules of Table 1, we find  $[U_{ab}$  is the matrix  $\rho(B_j)$  in the subspace with fixed  $a$

<sup>9</sup>Note that the references denote our  $0, \tau$  by  $*, p$ .

and  $b$ ]

$$\begin{aligned}
U_{00} = V_{00} = (\omega^{-1}); \quad U_{0\tau} &= \begin{pmatrix} \omega^{-2} & 0 \\ 0 & \omega^{-1} \end{pmatrix}, V_{0\tau} = \begin{pmatrix} \phi^{-1}\omega^2 & \phi^{-1/2}\omega \\ \phi^{-1/2}\omega & -\phi^{-1} \end{pmatrix}; \\
U_{\tau 0} = V_{0\tau}, V_{\tau 0} = U_{0\tau}; \quad U_{\tau\tau} &= \begin{pmatrix} \phi^{-1}\omega^2 & 0 & \phi^{-1/2}\omega \\ 0 & \omega^{-1} & 0 \\ \phi^{-1/2}\omega & 0 & -\phi^{-1} \end{pmatrix}, V_{\tau\tau} = \begin{pmatrix} \omega^{-1} & 0 & 0 \\ 0 & \phi^{-1}\omega^2 & \phi^{-1/2}\omega \\ 0 & \phi^{-1/2}\omega & -\phi^{-1} \end{pmatrix}.
\end{aligned} \tag{40}$$

Here, we have ordered the basis states as follows:  $\{|0, \tau, \tau, 0\rangle\}_{00}$ ,  $\{|0, \tau, 0, \tau\rangle, |0, \tau, \tau, \tau\rangle\}_{0\tau}$ ,  $\{|\tau, 0, \tau, 0\rangle, |\tau, \tau, \tau, 0\rangle\}_{\tau 0}$ , and  $\{|\tau, 0, \tau, \tau\rangle, |\tau, \tau, 0, \tau\rangle, |\tau, \tau, \tau, \tau\rangle\}_{\tau\tau}$ . It is now an easy exercise in matrix multiplication to verify  $UVU = VUV$  and thus to show that  $\rho_\tau$  is a unitary representation of the braid group.

We obtain more insights into the operations performed by braiding by choosing  $j = 1$ ,  $f_0 = 0$  and looking at the states  $|((\tau_1, \tau_2)_a, \tau_3)_b\rangle$  of the three Fibonacci anyons in Eq. (38). Performing  $B_1$  by braiding the first two anyons (corresponding to the matrices  $U_{0b}$ ), the states simply acquire the phases  $\omega^{-2} = e^{-4\pi i/5}$  (if  $a = 0$ ) and  $\omega^{-1} = e^{3\pi i/5}$  (if  $a = \tau$ ) depending only on their fusion outcome  $a$ , irrespective of the value of  $b$ .<sup>10</sup>

On the other hand, braiding the anyons  $\tau_2$  and  $\tau_3$  with  $B_2$  (corresponding to  $V_{0b}$ ) is not diagonal in this basis as the two anyons do not have a well-defined fusion outcome; in the alternative basis  $|(\tau_1, (\tau_2, \tau_3)_{a'})_b\rangle$  the operation  $B_2$  would be the simple phase factors  $\omega^{-1}, \omega^{-2}$  depending on  $a'$  as before. It is easy to check that  $V_{0\tau} = F^{-1}U_{0\tau}F$  with the transformation matrix

$$F = F^{-1} = \begin{pmatrix} \phi^{-1} & \phi^{-1/2} \\ \phi^{-1/2} & -\phi^{-1} \end{pmatrix}, \tag{41}$$

which corresponds to the basis transformation

$$|(\tau_1, (\tau_2, \tau_3)_\tau)_0\rangle = |((\tau_1, \tau_2)_\tau, \tau_3)_0\rangle, \tag{42}$$

$$|(\tau_1, (\tau_2, \tau_3)_0)_\tau\rangle = \phi^{-1}|((\tau_1, \tau_2)_0, \tau_3)_\tau\rangle + \phi^{-1/2}|((\tau_1, \tau_2)_\tau, \tau_3)_\tau\rangle,$$

$$|(\tau_1, (\tau_2, \tau_3)_\tau)_\tau\rangle = \phi^{-1/2}|((\tau_1, \tau_2)_0, \tau_3)_\tau\rangle - \phi^{-1}|((\tau_1, \tau_2)_\tau, \tau_3)_\tau\rangle, \tag{43}$$

also known as the  $F$ -move.

A single Fibonacci qubit is realized by three Fibonacci anyons  $\tau_1, \tau_2, \tau_3$  in the state  $|0, \tau, f, \tau\rangle$ . The states with  $f \in \{0, \tau\}$  form the logical qubit  $|\bar{0}\rangle, |\bar{1}\rangle$ . From the calculation in Eq. (40) we know that the gate  $U_{0\tau}$  with the phases  $e^{-\pi i/10 \pm 7\pi i/10}$  is performed while braiding the first two anyons. Up to the irrelevant (Abelian) factor,  $e^{-\pi i/10}$ , the braid corresponds to a rotation by  $\frac{7}{5}\pi \equiv 252^\circ$  around the  $z$ -axis of the Bloch sphere. Similarly, braiding anyons  $\tau_2$  and  $\tau_3$  yields the gate  $V_{0\tau}$  in a protected fashion. This gate is another rotation by  $252^\circ$  around an axis that corresponds to the basis transformation given by  $F$ . In terms of the Bloch sphere, the rotation  $V_{0\tau}$  is a rotation around the axis  $\mathbf{v} = (2\phi^{-3/2}, 0, \phi^{-2} - \phi^{-1})^T$ . Braiding the anyons  $\tau_1, \tau_2, \tau_3$ , arbitrary products of  $U_{0\tau}$  and  $V_{0\tau}$  can be implemented and all single qubit gates can be performed in a protected manner.

To understand the idea of Ref. [38] regarding how to implement two-qubit gates, we first have to appreciate another crucial property of anyon braiding: braiding the fusion product  $(\tau_1, \tau_2)_a$  as a composite object results in the same net effect as braiding the elementary object  $a$ . As a simple example, let us consider the states  $|0, \tau, a, b\rangle = |((\tau_1, \tau_2)_a, \tau_3)_b\rangle$  as before. As

<sup>10</sup>The corresponding phases are known as elements of the R-matrix.



seen in Fig. 6(a), the braid  $B = B_2 B_1^2 B_2$  moves the composite object  $(\tau_1, \tau_2)_a$  around  $\tau_3$  and is represented by  $W = \rho_\tau(B)$ . From Eq. (40), we obtain after a straightforward calculation the result<sup>11</sup>

$$W_{ab} = \begin{cases} 1, & a = 0, b = \tau, \\ \omega^{-4}, & a = \tau, b = 0, \\ \omega^{-2}, & a = \tau, b = \tau. \end{cases} \quad (44)$$

We observe that as expected moving two anyons which fuse to the vacuum ( $a = 0$ ) around another anyon does not change the state of the system. However, when the fusion outcome is another anyon ( $a = \tau$ ), the result is  $(U_{0\tau})^2$ .

The following procedure allows us to obtain a controlled two-qubit gate by braiding: first, we find a ‘weave’, i.e., a braid where only a single anyon is moved around two static anyons that is equivalent to a braid, which only involves the static anyons. It can be checked that the weave of the third anyon shown in Fig. 6(b) is equivalent to  $B_1^4$  of the first two anyons up to an error that is smaller than a percent. Having found such a weave by brute force search, a controlled gate can be obtained with the idea of the composite object explained above, see Fig. 6(c). As before, we encode two qubits in the states  $|\bar{a}, \bar{b}\rangle = |((\tau_1, \tau_2)_a, \tau_3)_\tau\rangle \otimes |((\tau_4, \tau_5)_b, \tau_6)_\tau\rangle$  of six Fibonacci anyons.<sup>12</sup> We use  $|\bar{b}\rangle$  (formed by anyons  $\tau_4, \tau_5, \tau_6$  in red) as the control qubit and  $|\bar{a}\rangle$  (formed by anyons  $\tau_1, \tau_2, \tau_3$  in black) as the target. As the state of the control qubit is given by the fusion outcome  $b$  of  $\tau_4, \tau_5$ , moving the two anyons together around the anyons of the target qubit does nothing as long as  $b = 0$  (in this case, they are equivalent to the vacuum that braids trivially). In order to obtain a controlled gate that does not change the state of  $|\bar{b}\rangle$ , we let the pair of anyons  $\tau_4, \tau_5$  perform the weave found above. In this case, the control anyons (up to a small error) remain unaffected and, provided that  $b = \tau$ , the operation  $U_4 = (U_{0\tau})^4 = \text{diag}(e^{2\pi i/5}, e^{-4\pi i/5})$  is performed on the target. As a result, the braid of Fig. 6(c) acting on two qubits entangles them by a controlled- $U_4$  gate. Together with the universal set of single qubit gates found before, all gates can be performed by braiding Fibonacci anyons and the anyons are *universal* for quantum computation. More information on Fibonacci anyons can be found, e.g., in Refs. [7, 12, 39, 40]. For a method to design efficient braids that approximate a target unitary, see Refs. [41, 42].

## 5 Conclusion

We have shown how non-Abelian anyons can be used for topological quantum computers. The computation is performed by the wordlines of the anyons forming knots in space-time. The outcome of the computation is the fusion result at the last step of the computation. The computation is topologically protected in the sense that the gates performed do not depend on the concrete trajectories of the anyons but only on the overall topology of the braid.

The discussion so far has been concerned only with zero temperature. At any finite

<sup>11</sup>It follows from  $V_{0\tau}(U_{0\tau})^2 V_{0\tau} = \text{diag}(1, \omega^{-2})$  and  $V_{00}(U_{00})^2 V_{00} = \omega^{-4}$ .

<sup>12</sup>In terms of our states  $|f_0, f_1, \dots\rangle$  where  $f_j$  denotes the fusion outcome of all the anyons to the left, we have to add another passive anyon, which fuses with  $\tau$  to the vacuum, in between the three anyons forming qubit  $a$  and the three anyons forming qubit  $b$ . As a result, we have the encoding  $|\bar{a}, \bar{b}\rangle = |0, \tau, a, \tau, 0, \tau, b, \tau\rangle$ . Without the additional fusion outcome 0 the value  $b$  would not denote the fusion outcome of the two anyons to the left of it.

temperature, there is a finite fraction  $\propto \exp(-\bar{M}/k_B T)$  of thermal anyons present in the system ( $\bar{M}$  is the gap protecting the topological phase). Those anyons braid in an unwanted, uncontrollable fashion around the anyons forming the qubit. As a result, the computation is dephased and fails. If topological quantum computation is so fragile with respect to temperature, why did we bother to discuss the ideas at length? The answer to this question has many facets. First and most importantly, non-Abelian anyons are an interesting new form of quantum matter. The study of the potential ways in which (quasi-)particles may braid, depending on the dimension of space, is an interesting and important question of basic physics research, even without applications to quantum computation.

Regarding the potential for quantum computation, the argument given above simply means that we have to employ error correction at some level. Non-Abelian anyons have inspired error correction for a long time and have led to the concept of topological codes [5]. In particular, even if there is no passive system that features Fibonacci anyons at zero temperature, we can imagine keeping a system actively in a topological state with non-Abelian anyons by constantly performing syndrome measurements [43, 44].

Regarding the parity-protected quantum computation with Majorana zero modes; even though the protocol strictly only works at zero temperatures, we may expect the Majorana qubit to have a rather long lifetime at finite temperature. Moreover, it has recently been shown that the non-Abelian nature of the Majorana zero modes allows for dedicated error protection protocols relying on their non-Abelian nature [45–48]. The study of systems where the elementary excitations are particles with exotic exchange statistics is still a very active field with many surprises to come. Presently, there is a big experimental push to realize Ising-anyons in the form of Majorana zero modes in superconductor-semiconductor heterostructures, see Ref. [49]. However, so far, no compelling evidence of particles with non-Abelian exchange statistics has ever been observed.

I want to thank Lisa Arndt and Alex Ziesen for carefully reading the manuscript and proposing changes that helped to considerably increase the readability of the text.

## Appendix

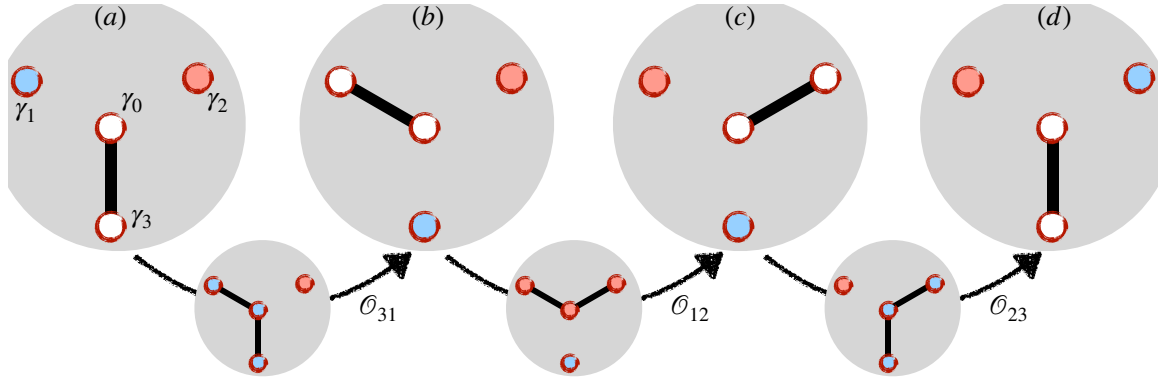


Figure 7: Steps to interchange the blue and red Majorana zero modes that are initially located at positions 1 and 2. The first move from (a) to (b) moves the blue Majorana zero mode from position 1 to position 3. In the first step (small circle below), the coupling between  $\gamma_0$  and  $\gamma_1$  is increased, which leads to the delocalization of the blue Majorana zero mode as a superposition of  $\gamma_1, \gamma_0, \gamma_3$ . In the second step, the coupling between  $\gamma_0$  and  $\gamma_3$  is reduced which moves the blue Majorana mode to position 3. In the step from (b) to (c), the red Majorana mode is moved from position 2 to position 1. In the last step, the blue Majorana mode is moved from position 3 to position 2.

## A Braiding of Majorana zero modes

In this appendix, we want to derive the unitary operation that is performed when exchanging two Majorana zero modes. We discuss this in a system consisting of four Majorana zero modes, which are aligned in a Y-junction [32, 50]. We call the Majorana modes at the three ends of the Y-junction  $\gamma_1, \gamma_2$ , and  $\gamma_3$ . The Majorana mode in the middle is denoted by  $\gamma_0$ . The Hamiltonian of the system assumes the form

$$H = i \sum_{j=1}^3 \epsilon_j \gamma_0 \gamma_j = i \gamma_0 (\boldsymbol{\epsilon} \cdot \boldsymbol{\gamma}) \quad (45)$$

with  $\epsilon_j$  as three parameters that give the coupling strength of the two Majorana modes on each leg of the junction. Slowly tuning these couplings in a controlled fashion makes it possible to interchange Majorana modes, and thus we can observe the non-Abelian statistics. In particular, we would like to study the situation in Fig. 7.

We start at time (a) with  $\epsilon_3 = \bar{\epsilon}$  and  $\epsilon_1 = \epsilon_2 = 0$ . Then we increase  $\epsilon_1$  to  $\bar{\epsilon}$  and afterwards decrease  $\epsilon_3$  to 0 such that at time (b) we have moved the blue Majorana zero mode to the bottom (from position 1 to position 3). To finish the exchange, we perform the same procedure from position 2 to position 1 and finally, from position 3 to position 2.

## A.1 Non-Abelian Berry phase

The Berry phase is a geometric phase that arises when a parameter of the Hamiltonian is changed slowly, and we want to observe the change in the ground state wavefunction. In the case where the ground state is degenerate, the change in the parameter might induce transitions between the different degenerate states, leading to a non-Abelian Berry phase which is generated by the non-Abelian gauge field

$$A_{ab}^k = i \langle \psi_a(\epsilon) | \partial_{\epsilon_k} | \psi_b(\epsilon) \rangle; \quad (46)$$

here,  $\psi_a(\epsilon)$  denotes the different degenerate ground state wavefunctions for the Hamiltonian with parameters  $\epsilon$ .

Changing the parameter along a contour  $\epsilon(s)$ , the ground states are transformed according to the unitary matrix

$$U = \mathcal{P} \exp \left( i \int \mathbf{A} \cdot d\epsilon \right) \quad (47)$$

where  $\mathcal{P}$  denotes the path ordering.

A basis-independent way to obtain the evolution of the ground state due to Kato is the following [51]: given the projector  $P(\epsilon)$  onto the ground state manifold (which depends on the parameters  $\epsilon$ ), we define the Kato Hamiltonian

$$K^k = i [P(\epsilon), \partial_{\epsilon_k} P(\epsilon)] \quad (48)$$

with which the unitary evolution in Eq. (47) can be written as

$$U_K = \mathcal{P} \exp \left( i \int \mathbf{K} \cdot d\epsilon \right). \quad (49)$$

It can be shown that  $U_K = U$  for any closed contour [52].

## A.2 Calculating the non-Abelian Berry phase

The Hamiltonian  $H$  has the eigenenergies  $\pm\epsilon$  ( $\epsilon = |\epsilon|$ ) where both of them are doubly degenerate. For the Berry phase, we need to project onto the ground state sector on which  $H = -\epsilon$ . The projector is given by

$$P(\epsilon) = \frac{1}{2\epsilon} (\epsilon - H) = \frac{1}{2\epsilon} [\epsilon - i\gamma_0(\epsilon \cdot \boldsymbol{\gamma})] \quad (50)$$

which leads to

$$\partial_{\epsilon_k} P(\epsilon) = \frac{i\gamma_0}{2\epsilon^3} \sum_{j \neq k} (\epsilon_k \epsilon_j \gamma_j - \epsilon_j^2 \gamma_k). \quad (51)$$



Now it is straightforward to calculate the Kato Hamiltonian

$$\begin{aligned}
K^k &= \frac{i}{4\epsilon^4} \sum_i \sum_{j \neq k} \epsilon_i \left( \epsilon_k \epsilon_j \overbrace{[\gamma_0 \gamma_i, \gamma_0 \gamma_j]}^{2(\delta_{ij}-1)\gamma_i \gamma_j} - \epsilon_j^2 \overbrace{[\gamma_0 \gamma_i, \gamma_0 \gamma_k]}^{2(\delta_{ik}-1)\gamma_i \gamma_k} \right) \\
&= \frac{i}{2\epsilon^4} \left[ \sum_{j \neq k} \epsilon_j^2 \sum_{i \neq k} \epsilon_i \gamma_i \gamma_k - \epsilon_k \sum_{i \neq j} \sum_{j \neq k} \epsilon_i \epsilon_j \gamma_i \gamma_j \right] \\
&= \frac{i}{2\epsilon^4} \left[ (\epsilon^2 - \epsilon_k^2) (\mathbf{e} \cdot \boldsymbol{\gamma} - \epsilon_k \gamma_k) \gamma_k + \epsilon_k^2 (\mathbf{e} \cdot \boldsymbol{\gamma} - \epsilon_k \gamma_k) \gamma_k \right] \\
&= \frac{i}{2\epsilon^2} (\mathbf{e} \cdot \boldsymbol{\gamma} - \epsilon_k \gamma_k) \gamma_k. \tag{52}
\end{aligned}$$

The result when changing a single parameter reads

$$\begin{aligned}
i \int_{\epsilon_{\text{start}}}^{\epsilon_{\text{stop}}} d\epsilon_k K^k &= \overbrace{(\epsilon_k \gamma_k - \mathbf{e} \cdot \boldsymbol{\gamma}) \gamma_k}^{= -\sum_{j \neq k} \epsilon_j \gamma_j \text{ (indep. of } \epsilon_k)} \times \int_{\epsilon_{\text{start}}}^{\epsilon_{\text{stop}}} \frac{d\epsilon_k}{2\epsilon^2} \\
&= \frac{1}{2\epsilon_{\perp}} \arctan(\epsilon_k / \epsilon_{\perp}) \Big|_{\epsilon_{\text{start}}}^{\epsilon_{\text{stop}}} \tag{53}
\end{aligned}$$

with  $\epsilon_{\perp} = \left( \sum_{j \neq k} \epsilon_j^2 \right)^{1/2}$ .

A braid is constructed from elementary moves, see Fig. 7. We exemplify the calculation of  $\mathcal{O}_{31}$ . Starting with  $\epsilon_3 = \bar{\epsilon}$  and  $\epsilon_1 = \epsilon_2 = 0$ , we first turn on  $\epsilon_1$  from 0 to  $\bar{\epsilon}$  which yields ( $k = 1, \epsilon_{\text{start}} = 0, \epsilon_{\text{stop}} = \bar{\epsilon}$ )

$$U_a = \exp\left(-\bar{\epsilon} \gamma_3 \gamma_1 \times \frac{1}{2\bar{\epsilon}} \frac{\pi}{4}\right) = \exp\left(\frac{\pi}{8} \gamma_1 \gamma_3\right).$$

In the second step, we start with  $\epsilon_1 = \epsilon_3 = \bar{\epsilon}$  and  $\epsilon_2 = 0$  and reduce  $\epsilon_3$  down to 0. This step yields a non-Abelian Berry phase ( $k = 3, \epsilon_{\text{start}} = \bar{\epsilon}, \epsilon_{\text{stop}} = 0$ )

$$U_b = \exp\left(-\bar{\epsilon} \gamma_1 \gamma_3 \times -\frac{1}{2\bar{\epsilon}} \frac{\pi}{4}\right) = \exp\left(\frac{\pi}{8} \gamma_1 \gamma_3\right).$$

So all together, we have the transformation

$$\mathcal{O}_{31} = U_b U_a = \exp\left(\frac{\pi}{4} \gamma_1 \gamma_3\right) = \frac{1}{\sqrt{2}} (1 + \gamma_1 \gamma_3) \tag{54}$$

from (a) to (b) that moves the Majorana zero mode from position 1 to position 3. The whole operation of exchanging the particles 1 and 2 is given by

$$\rho_{\gamma}(B_1) = \mathcal{O}_{23} \mathcal{O}_{12} \mathcal{O}_{31} = \frac{1}{2^{3/2}} (1 + \gamma_3 \gamma_2) (1 + \gamma_2 \gamma_1) (1 + \gamma_1 \gamma_3) = \frac{1}{\sqrt{2}} (1 - \gamma_1 \gamma_2) = e^{-\frac{\pi}{4} \gamma_1 \gamma_2}. \tag{55}$$

The braiding operation  $\rho(B_1)$  transforms the Majorana zero modes as

$$\gamma_1 \mapsto \rho_{\gamma}(B_1) \gamma_1 \rho_{\gamma}(B_1)^{\dagger} = \gamma_2, \quad \gamma_2 \mapsto \rho_{\gamma}(B_1) \gamma_2 \rho_{\gamma}(B_1)^{\dagger} = -\gamma_1. \tag{56}$$

It is a natural question to ask which of the two modes  $\gamma_1$  or  $\gamma_2$  gets a minus sign. It turns out that in our setting of Fig. 7,  $\gamma_2$  obtains a minus sign (it is transformed to  $-\gamma_1$ ) as it is

only moved once in the second step ( $\mathcal{O}_{12}$ ). On the other hand,  $\gamma_1$  is moved twice, in the first step ( $\mathcal{O}_{31}$ ) and in the last step ( $\mathcal{O}_{32}$ ). Indeed, in a single step, we have

$$\mathcal{O}_{31}\gamma_1\mathcal{O}_{31}^\dagger = -\gamma_3 \quad (57)$$

and thus  $\gamma_1$  is moved to  $-\gamma_3$ . As a result, we would obtain the conjugate representation  $\rho_\gamma(B_1) = e^{\frac{\pi}{4}\gamma_1\gamma_2}$ , which is often employed in the literature, if the geometry in Fig. 7 would look like a ‘ $\lambda$ ’ rather than a ‘Y’.

---

## References

- [1] R. Hanbury Brown and R. Q. Twiss, A test of a new type of stellar interferometer on Sirius, *Nature* **178**, 1046 (1956), doi:[10.1038/1781046a0](https://doi.org/10.1038/1781046a0).
- [2] E. Brannen and H. I. S. Ferguson, The question of correlation between photons in coherent light rays, *Nature* **178**, 481 (1956), doi:[10.1038/178481a0](https://doi.org/10.1038/178481a0).
- [3] I. Silva and O. Freire, Jr., The concept of the photon in question, *Hist. Stud. Nat. Sci.* **43**, 453 (2013), doi:[10.1525/hsns.2013.43.4.453](https://doi.org/10.1525/hsns.2013.43.4.453).
- [4] M. H. Freedman, M. Larsen, and Z. Whang, A modular functor which is universal for quantum computation, *Commun. Math. Phys.* **227**, 605 (2002), doi:[10.1007/s002200200645](https://doi.org/10.1007/s002200200645).
- [5] A. Yu. Kitaev, Fault-tolerant quantum computation by anyons, *Ann. Phys. (N. Y.)* **303**, 2 (2003), doi:[10.1016/S0003-4916\(02\)00018-0](https://doi.org/10.1016/S0003-4916(02)00018-0).
- [6] P. A. M. Dirac, Quantised singularities in the electromagnetic field, *Proc. R. Soc. A* **133**, 60 (1931), doi:[10.1098/rspa.1931.0130](https://doi.org/10.1098/rspa.1931.0130).
- [7] J. Preskill, *Lecture notes: Quantum computation*, chapter 9 (2004).
- [8] J. Alicea, New directions in the pursuit of Majorana fermions in solid state systems, *Rep. Prog. Phys.* **75**, 076501 (2012), doi:[10.1088/0034-4885/75/7/076501](https://doi.org/10.1088/0034-4885/75/7/076501).
- [9] M. Leijnse and K. Flensberg, Introduction to topological superconductivity and Majorana fermions, *Semicond. Sci. Technol.* **27**, 124003 (2012), doi:[10.1088/0268-1242/27/12/124003](https://doi.org/10.1088/0268-1242/27/12/124003).
- [10] C. W. J. Beenakker, Search for Majorana fermions in superconductors, *Annu. Rev. Con. Mat. Phys.* **4**, 113 (2013), doi:[10.1146/annurev-conmatphys-030212-184337](https://doi.org/10.1146/annurev-conmatphys-030212-184337).
- [11] J. K. Pachos, *Introduction to topological quantum computation* (Cambridge University Press, Cambridge, 2012).
- [12] C. Nayak, S. H. Simon, A. Stern, M. Freedman, and S. Das Sarma, Non-Abelian anyons and topological quantum computation, *Rev. Mod. Phys.* **80**, 1083 (2008), doi:[10.1103/RevModPhys.80.1083](https://doi.org/10.1103/RevModPhys.80.1083).
- [13] A. Stern and N. H. Lindner, Topological quantum computation—from basic concepts to first experiments, *Science* **339**, 1179 (2013), doi:[10.1126/science.1231473](https://doi.org/10.1126/science.1231473).
- [14] S. Das Sarma, M. Freedman, and C. Nayak, Majorana zero modes and topological quantum computation, *npj Quantum Inf.* **1**, 15001 (2015), doi:[10.1038/npjqi.2015.1](https://doi.org/10.1038/npjqi.2015.1).
- [15] R. Jackiw and C. Rebbi, Solitons with fermion number 1/2, *Phys. Rev. D* **13**, 3398 (1976), doi:[10.1103/PhysRevD.13.3398](https://doi.org/10.1103/PhysRevD.13.3398).
- [16] A. Yu. Kitaev, Unpaired Majorana fermions in quantum wires, *Phys.-Usp.* **44** (suppl.), 131 (2001), doi:[10.1070/1063-7869/44/10S/S29](https://doi.org/10.1070/1063-7869/44/10S/S29).

- 
- [17] R. P. Feynman, R. B. Leighton, and M. Sands, *Feynman lectures on physics: Quantum mechanics*, vol. 3 (Addison-Wesley, Reading, 1965).
- [18] B. M. Terhal and D. P. DiVincenzo, Classical simulation of noninteracting-fermion quantum circuits, *Phys. Rev. A* **65**, 032325 (2002), doi:[10.1103/PhysRevA.65.032325](https://doi.org/10.1103/PhysRevA.65.032325).
- [19] C. W. J. Beenakker, D. P. DiVincenzo, C. Emary, and M. Kindermann, Charge detection enables free-electron quantum computation, *Phys. Rev. Lett.* **93**, 020501 (2004), doi:[10.1103/PhysRevLett.93.020501](https://doi.org/10.1103/PhysRevLett.93.020501).
- [20] F. Hassler, Majorana qubits, in *Quantum Information Processing. Lecture Notes of the 44th IFF Spring School*, edited by D. P. DiVincenzo (Verlag des Forschungszentrums Jülich, 2013).
- [21] Z.-C. Gu and X.-G. Wen, Tensor-entanglement-filtering renormalization approach and symmetry protected topological order, *Phys. Rev. B* **80**, 155131 (2009), doi:[10.1103/PhysRevB.80.155131](https://doi.org/10.1103/PhysRevB.80.155131).
- [22] F. Pollmann, E. Berg, A. M. Turner, and M. Oshikawa, Symmetry protection of topological order in one-dimensional quantum spin systems, *Phys. Rev. B* **85**, 075125 (2012), doi:[10.1103/PhysRevB.85.075125](https://doi.org/10.1103/PhysRevB.85.075125).
- [23] F. Hassler, A. R. Akhmerov, and C. W. J. Beenakker, Top-transmon: Hybrid superconducting qubit for parity-protected quantum computation, *New J. Phys.* **13**, 095004 (2011), doi:[10.1088/1367-2630/13/9/095004](https://doi.org/10.1088/1367-2630/13/9/095004).
- [24] A. Kitaev, Anyons in an exactly solved model and beyond, *Ann. Phys. (N. Y.)* **321**, 2 (2006), doi:[10.1016/j.aop.2005.10.005](https://doi.org/10.1016/j.aop.2005.10.005).
- [25] A. Stern, Anyons and the quantum Hall effect—a pedagogical review, *Ann. Phys. (N. Y.)* **323**, 204 (2008), doi:[10.1016/j.aop.2007.10.008](https://doi.org/10.1016/j.aop.2007.10.008).
- [26] F. Wilczek, Magnetic flux, angular momentum, and statistics, *Phys. Rev. Lett.* **48**, 1144 (1982), doi:[10.1103/PhysRevLett.48.1144](https://doi.org/10.1103/PhysRevLett.48.1144).
- [27] E. Artin, Theory of braids, *Ann. Math.* **48**, 101 (1947), doi:[10.2307/1969218](https://doi.org/10.2307/1969218).
- [28] N. Read and D. Green, Paired states of fermions in two dimensions with breaking of parity and time-reversal symmetries, and the fractional quantum Hall effect, *Phys. Rev. B* **61**, 10267 (2000), doi:[10.1103/PhysRevB.61.10267](https://doi.org/10.1103/PhysRevB.61.10267).
- [29] D. A. Ivanov, Non-Abelian statistics of half-quantum vortices in p-wave superconductors, *Phys. Rev. Lett.* **86**, 268 (2001), doi:[10.1103/PhysRevLett.86.268](https://doi.org/10.1103/PhysRevLett.86.268).
- [30] J. Alicea, Y. Oreg, G. Refael, F. von Oppen, and M. P. A. Fisher, Non-Abelian statistics and topological quantum computation in 1D wire networks, *Nat. Phys.* **7**, 412 (2011), doi:[10.1038/nphys1915](https://doi.org/10.1038/nphys1915).
- [31] D. J. Clarke, J. D. Sau, and S. Tewari, Majorana fermion exchange in quasi-one-dimensional networks, *Phys. Rev. B* **84**, 035120 (2011), doi:[10.1103/PhysRevB.84.035120](https://doi.org/10.1103/PhysRevB.84.035120).

- 
- [32] B. van Heck, A. R. Akhmerov, F. Hassler, M. Burrello, and C. W. J. Beenakker, Coulomb-assisted braiding of Majorana fermions in a Josephson junction array, *New J. Phys.* **14**, 035019 (2012), doi:[10.1088/1367-2630/14/3/035019](https://doi.org/10.1088/1367-2630/14/3/035019).
- [33] B. I. Halperin, Y. Oreg, A. Stern, G. Refael, J. Alicea, and F. von Oppen, Adiabatic manipulations of Majorana fermions in a three-dimensional network of quantum wires, *Phys. Rev. B* **85**, 144501 (2012), doi:[10.1103/PhysRevB.85.144501](https://doi.org/10.1103/PhysRevB.85.144501).
- [34] D. Aasen, M. Hell, R. V. Mishmash, A. Higginbotham, J. Danon, M. Leijnse, T. S. Jespersen, J. A. Folk, C. M. Marcus, K. Flensberg, and J. Alicea, Milestones toward Majorana-based quantum computing, *Phys. Rev. X* **6**, 031016 (2016), doi:[10.1103/PhysRevX.6.031016](https://doi.org/10.1103/PhysRevX.6.031016).
- [35] S. Bravyi and A. Yu. Kitaev, Universal quantum computation with ideal Clifford gates and noisy ancillas, *Phys. Rev. A* **71**, 022316 (2005), doi:[10.1103/PhysRevA.71.022316](https://doi.org/10.1103/PhysRevA.71.022316).
- [36] L. H. Kauffman and S. J. Lomonaco, Jr.,  $q$  — Deformed spin networks, knot polynomials and anyonic topological quantum computation, *J. Knot Theory Ramif.* **16**, 267 (2007), doi:[10.1142/S0218216507005282](https://doi.org/10.1142/S0218216507005282).
- [37] P. W. Shor and S. P. Jordan, Estimating Jones polynomials is a complete problem for one clean qubit, *Quantum Inf. Comput.* **8**, 681 (2008), doi:[10.26421/QIC8.8-9-1](https://doi.org/10.26421/QIC8.8-9-1).
- [38] N. E. Bonesteel, L. Hormozi, G. Zikos, and S. H. Simon, Braid topologies for quantum computation, *Phys. Rev. Lett.* **95**, 140503 (2005), doi:[10.1103/PhysRevLett.95.140503](https://doi.org/10.1103/PhysRevLett.95.140503).
- [39] L. Hormozi, G. Zikos, N. E. Bonesteel, and S. H. Simon, Topological quantum compiling, *Phys. Rev. B* **75**, 165310 (2007), doi:[10.1103/PhysRevB.75.165310](https://doi.org/10.1103/PhysRevB.75.165310).
- [40] S. Trebst, M. Troyer, Z. Wang, and A. W. W. Ludwig, A short introduction to Fibonacci anyon models, *Prog. Theor. Phys. Supp.* **176**, 384 (2008), doi:[10.1143/PTPS.176.384](https://doi.org/10.1143/PTPS.176.384).
- [41] M. Burrello, H. Xu, G. Mussardo, and X. Wan, Topological Quantum Hashing with the Icosahedral Group, *Phys. Rev. Lett.* **104**, 160502 (2010), doi:[10.1103/PhysRevLett.104.160502](https://doi.org/10.1103/PhysRevLett.104.160502).
- [42] M. Burrello, G. Mussardo and X. Wan, Topological quantum gate construction by iterative pseudogroup hashing, *New J. Phys.* **13**, 025023 (2011), doi:[10.1088/1367-2630/13/2/025023](https://doi.org/10.1088/1367-2630/13/2/025023).
- [43] R. Koenig, G. Kuperberg, and B. W. Reichardt, Quantum computation with Turaev-Viro codes, *Ann. Phys. (N. Y.)* **325**, 2707 (2010), doi:[10.1016/j.aop.2010.08.001](https://doi.org/10.1016/j.aop.2010.08.001).
- [44] N. E. Bonesteel and D. P. DiVincenzo, Quantum circuits for measuring Levin-Wen operators, *Phys. Rev. B* **86**, 165113 (2012), doi:[10.1103/PhysRevB.86.165113](https://doi.org/10.1103/PhysRevB.86.165113).
- [45] B. M. Terhal, F. Hassler, and D. P. DiVincenzo, From Majorana fermions to topological order, *Phys. Rev. Lett.* **108**, 260504 (2012), doi:[10.1103/PhysRevLett.108.260504](https://doi.org/10.1103/PhysRevLett.108.260504).
- [46] S. Vijay, T. H. Hsieh, and L. Fu, Majorana fermion surface code for universal quantum computation, *Phys. Rev. X* **5**, 041038 (2015), doi:[10.1103/PhysRevX.5.041038](https://doi.org/10.1103/PhysRevX.5.041038).

- 
- [47] S. Plugge, L. A. Landau, E. Sela, A. Altland, K. Flensberg, and R. Egger, Roadmap to Majorana surface codes, *Phys. Rev. B* **94**, 174514 (2016), doi:[10.1103/PhysRevB.94.174514](https://doi.org/10.1103/PhysRevB.94.174514).
- [48] D. Litinski, M. S. Kesselring, J. Eisert, and F. von Oppen, Combining topological hardware and topological software: Color code quantum computing with topological superconductor networks, *Phys. Rev. X* **7**, 031048 (2017), doi:[10.1103/PhysRevX.7.031048](https://doi.org/10.1103/PhysRevX.7.031048).
- [49] E. Prada, P. San-Jose, M. W. A. de Moor, A. Geresdi, E. J. H. Lee, J. Klinovaja, D. Loss, J. Nygård, R. Aguado, and L. P. Kouwenhoven, From Andreev to Majorana bound states in hybrid superconductor-semiconductor nanowires, *Nat. Rev. Phys.* **2**, 575 (2020), doi:[10.1038/s42254-020-0228-y](https://doi.org/10.1038/s42254-020-0228-y)
- [50] J. D. Sau, D. J. Clarke, and S. Tewari, Controlling non-Abelian statistics of Majorana fermions on Majorana dimer lattices, *Phys. Rev. B* **84**, 094505 (2011), doi:[10.1103/PhysRevB.84.094505](https://doi.org/10.1103/PhysRevB.84.094505).
- [51] T. Kato, On the adiabatic theorem of quantum mechanics, *J. Phys. Soc. Jap.* **5**, 435 (1950), doi:[10.1143/JPSJ.5.435](https://doi.org/10.1143/JPSJ.5.435).
- [52] J. E. Avron, L. Sadun, J. Seger, and B. Simon, Chern numbers, quaternions, and Berry's phases in Fermi systems, *Commun. Math. Phys.* **124**, 595 (2009), doi:[10.1007/BF01218452](https://doi.org/10.1007/BF01218452).